

## FABRICATION, CHARACTERIZATION, AND *IN VITRO* EVALUATION OF PEGYLATED GLYCERIDE LABRASOL® NANOSTRUCTURED LIPID CARRIER COMPOSITES OF METHOTREXATE: THE PATHWAY TO EFFECTIVE CANCER THERAPY

RADHARANI PANDA, KETOUSU KUOTSU\*

Department of Pharmaceutical Technology, Division of Pharmaceutics, Jadavpur University, Kolkata, West Bengal, India.  
Email: ketousetuokuotsu18@yahoo.com

Received: 03 April 2019, Revised and Accepted: 30 April 2019

### ABSTRACT

**Objective:** The objective of the current study is to optimize and evaluate the potential of polyethylene glycolylated (PEG) glyceride Labrasol® nanostructured lipid carrier (NLC) composites of methotrexate (MTX) to achieve enhanced sustained release delivery in cancer treatment.

**Materials and Methods:** MTX-NLC was successfully prepared by hot melt emulsification and probe sonication method for spatial and controlled release of this therapeutic agent.

**Results:** The solubility screening of MTX and lipids resulted in the selection of Monostearin as solid lipid, PEGylated glyceride Labrasol® and olive oil as liquid lipids for the formulation of MTX-loaded NLC composites. Particle size, zeta potential, and polydispersity index of both the composites were confirmed using dynamic light scattering, whereby Labrasol® MTX-NLC showed high entrapment efficiency and drug loading. A spherical particle shape with smooth surface of all the composites was confirmed from the scanning electron microscope and transmission electron microscopy analysis. Labrasol® MTX-NLC showed remarkably increased cytotoxic response, augmented cellular uptake, and low half maximal inhibitory concentration value in MCF-7 cells. *In vitro* release study confirmed that encapsulation of MTX in PEGylated glyceride Labrasol® MTX-NLC resulted in enhanced sustained release of MTX for a period of 48 h.

**Conclusion:** The present study establishes that PEGylated glyceride Labrasol® MTX-NLC can be considered as a promising anticancer delivery system, thereby improving antitumor efficacy of the drug.

**Keywords:** Methotrexate, Nanostructured lipid carrier, Polyethylene glycolylated glyceride, *In vitro* release, MCF-7 cells, Half maximal inhibitory concentration value, Cellular uptake.

© 2019 The Authors. Published by Innovare Academic Sciences Pvt Ltd. This is an open access article under the CC BY license (<http://creativecommons.org/licenses/by/4.0/>) DOI: <http://dx.doi.org/10.22159/ajpcr.2019.v12i6.33377>

### INTRODUCTION

In the current scenario, cancer is one of the most leading causes of morbidity and mortality developing in any commonality at any point of time [1,2]. In addition, the productiveness of the present standard therapies for cancer is insignificant as the cytotoxic agents are highly toxic, low specificity with narrow therapeutic window and demonstrate short biological half-lives [3]. However, due to the origination of highly efficient therapeutic tools, delivery technologies and the availability of improved comprehension on cancer biology lead to remarkable enhancement of cancer survival rate [4].

Methotrexate (MTX), a folate antagonist which competitively binds to dihydrofolate reductase enzyme thereby hampers the growth of the cell and arrests the cell division cycle in G1 phase and S phase (Fig. 1). It is used as a chemotherapeutic agent in the treatment of different tumors such as osteosarcoma, breast cancer, acute lymphoblastic leukemia, and head, neck, and lung cancer [5]. However, MTX has restricted clinical implementations due to its low solubility, short biological half-life, dose-related cytotoxicity, and cellular efflux [6].

A classic therapeutic drug delivery system for cytotoxics must be formulated using the US Food and Drug Administration approved components and has acquired the generally recognized as safe status for both pharmaceutical and medicinal usage [7-9]. Over the past few years, extensive research has been carried out in nanotechnological field comprising polymers or lipids [10]. Profound research has been carried out on nanotechnology in the design and development of potent cytotoxic therapeutic cargo carriers to solve various issues related to

solubility and bioavailability of these therapeutics. These nanoparticles ultimately enhance the therapeutic efficacy by accurately transporting the drug cargo carrying the cytotoxics to the tumors and successfully safeguarding the drug carrier from biological conditions [11,12]. Furthermore, the enhanced permeability and retention effect of the tumor vasculature allows these nanoparticles to passively target the tumor and the suppressed lymphatic filtration allows them to retain at the specific site [13,14].

Lipid-based nanoparticles have been used as an efficient carrier for therapeutics for several years [15,16]. Due to the presence of biodegradable and biocompatible natural ingredients, these nanocomposites have greatly achieved importance as feasible substitutes to the polymeric nanoparticles [17]. These nanoparticles possess unique physicochemical characteristics, for which it can be prepared easily with the use of melt emulsification method of the lipids and subsequent recrystallization, thus circumventing the usage of possibly harmful organic solvents which are frequently used in polymeric nanoparticle formulations [18,19].

Among various categories of lipid nanoparticles available, the nanostructured lipid carriers (NLCs) comprising mixture of both solid and liquid (like dispersed oils in triglycerides) lipids are considered as the latest or second generation of lipid-based nanopatform [20,21]. It possesses increased encapsulation efficacy in comparison to the first-generation solid lipid nanoparticles (SLNs) due to the presence of unstructured matrix emerged by the addition of liquid lipid to the solid lipid matrix which curbs the expulsion of therapeutics [22-24]. NLCs

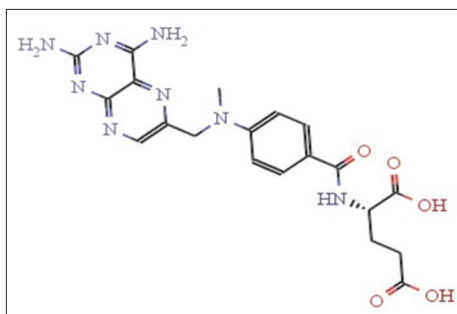


Fig. 1: Molecular structure of methotrexate

have been used multiple times as carrier for cytotoxic agents to induce tumor-specific targeting while overcoming multidrug resistance (MDR) and avoiding reticuloendothelial system clearance of therapeutics, thereby augmenting the anticancer efficacy of NLCs at the site of action [25].

High lipophilicity property of MTX makes it an efficient cargo to be encapsulated in the NLC, thereby maintaining the stability. Due to the opsonization process, lipidic nanocarriers after injection get discharged inevitably from the bloodstream and by the mononuclear phagocytic system get eliminated from the blood circulation [26]. Recently, different efforts were made to incorporate modified glycerides with hydrophilic moieties as polyethylene glycol (PEG) (e.g. Labrasol®) into the NLC formulations and have evaluated their practicability to form lipid matrix structure [27]. In Labrasol® (PEG-8 caprylic/capric glycerides) which is caprylocaproyl macrogol-8 glycerides, the PEG moiety in this oily vehicle is coupled with hydrophobic molecules resulting in its emulsifying features [28]. It offers novel dual activity as an excipient in the NLC carrier, primarily as an oily component and second as the PEG-containing substrate, thereby enhancing the biological half-life of the therapeutic and increasing the storage stability of nanocomposites [29]. Thus, the rationale of the study was to formulate MTX-loaded colloidal NLCs using PEGylated glyceride Labrasol® and olive oil with disclosed benefits, thereby increasing the solubility of the drug. Furthermore, it protects the drug from degradation and reduces the renal clearance, thereby increasing its half-life in bloodstream. In addition, it augments the payload of MTX in NLCs, thereby allowing the sustained release delivery.

The objective of the present study was to design, fabricate, and optimize MTX-loaded NLCs using PEG-8 caprylic/capric glyceride (Labrasol®) as PEGylated glyceride and olive oil as non-PEGylated liquid lipid with Monostearin as solid lipid using hot melt emulsification and probe sonication production technique to assess their superiority over SLNs in terms of drug encapsulation efficacy, drug release properties, and storage stabilities. The anticancer efficacy of the optimized MTX-loaded NLCs was studied on breast cancer (MCF7) cell line. Hence, the novelty of the current study is to formulate novel NLC composites of MTX using Labrasol® (a PEGylated glyceride) and olive oil, to assess their sustained release effect and increased antitumor property.

## MATERIALS AND METHODS

### Materials

MTX was received as a gift from Cipla Ltd. (Goa, India). Monostearin (glycerol monostearate) and Tween 80 (polyoxyethylene sorbitan monooleate) were procured from Thermo Fisher Scientific India Pvt. Ltd. (Mumbai, India). Labrasol® (PEG-8 caprylic/capric glycerides) was provided by Gattefosse (Saint-Priest, France) as gift sample. Olive oil was purchased from Bertolli (Italy). Poloxamer 188 (Pluronic F68) was received as gift samples from BASF (USA). All other chemicals and solvents used were of analytical grade. The simulated gastric fluid and simulated intestinal fluid were prepared by following the official methods as described in the United States Pharmacopoeia (XXV).

## Methods

### Screening of a binary mixture of solid and liquid lipid phase

Depending on the parameter such as encapsulation efficiency (EE), solid and liquid lipid ratios were optimized. Therefore, six ratios of binary mixture of solid phase (Monostearin) and liquid phase (Labrasol®) were selected arbitrarily (90:10, 80:20, 70:30, 60:40, 50:50, and 40:60). The same ratios were selected again for the screening of another combination of binary mixture of solid lipid (Monostearin) and liquid lipid (olive oil) phase.

### Selection of surfactants

The concentration of surfactant was optimized by formulating NLC formulations using Poloxamer 188 in ascending order (1% w/w, 2% w/w, 5% w/w, and 10% w/w) of concentration by keeping other variables constant. Then, the size of particles and EE were evaluated to determine the optimized concentration of the surfactant for the formulation of NLC.

### Preparation of MTX-NLCs

The MTX-NLCs were formulated using hot melt emulsification and probe sonication technique which shows the superiority over other processes as it is one of the most cost-effective and less time-consuming processes for the production of NLC formulations [30]. Briefly, the lipid phase comprised Monostearin and Labrasol® along with MTX which were melted beyond 81°C with continuous stirring in a beaker on a hot plate magnetic stirrer (Tarsons Products Pvt. Ltd., Kolkata, India). The aqueous phase consisting of deionized water and Poloxamer 188 was taken in another beaker and temperature was maintained similar to that of the above-melted lipid mixture. To the lipid phase mixture, heated aqueous mixture was added under continuous stirring at 600 rpm and heated using hot plate magnetic stirrer to form a primary microemulsion. It was then homogenized using a homogenizer (Ultra Turrax® T10, IKA) at 10,000 rpm for 5 min then subjected to probe sonication at 2 min interval for 10 min at 75% amplitude. NLCs containing olive oil as liquid lipid were also formulated following the above procedure. The preparation method of the blank NLCs was similar only without MTX. Then, the hot NLC dispersion was kept at 25°C for cooling to allow lipid solidification and to achieve the desired NLC composites.

### Physicochemical characterization of the formulated MTX-NLCs

Evaluation of particle size (PS), polydispersity index (PDI), and zeta potential

By the utilization of dynamic light scattering (DLS) technology, the average PS, size distribution pattern, and PDI of NLCs were evaluated in a Zetasizer Nano ZS90 analyzer (Malvern Instruments, Malvern, UK). Whereas, depending on the electrophoretic mobility in the presence of the electric field, the zeta potential was measured. The NLCs suspension was then vortexed after diluting with deionized water to bypass the phenomena of multiple scattering, kept in polystyrene cuvettes for the evaluation of all the above parameters.

### Determination of drug EE% and drug loading (DL%) efficiency

Both EE% and DL% of MTX in the formulated NLCs were calculated using ultrafiltration method [31]. MTX-NLC dispersion of 0.5 ml was poured into an ultrafiltration centrifuge tubes and then subjected to centrifugation (Remi CPR-24) at 9000 rpm for 40 min. Then, the amount of free MTX present in the ultrafiltrate was quantified spectrophotometrically at  $\lambda_{max}$  302 nm using ultraviolet/visible (UV/VIS) spectrophotometer (JASCO V-550) using 1 cm quartz cells. Each experiment was carried out in triplicates.

The EE% and DL% were calculated by the following equations:

$$\text{Encapsulation efficiency (EE\%)} = \left( \frac{W_{\text{total}} - W_{\text{free}}}{W_{\text{total}}} \right) \times 100$$

$$\text{Durg loading efficiency (DL\%)} = \left( \frac{W_{\text{total}} - W_{\text{free}}}{W_{\text{Lipid}}} \right) \times 100$$

Where,  $W_{\text{total}}$  was the amount of the total MTX in NLC,  $W_{\text{free}}$  was the amount of unencapsulated MTX remaining in ultrafiltrate, and  $W_{\text{Lipid}}$  was the total amount of the lipid in the NLC composite.

#### Fourier-transform infrared (FTIR) spectroscopy

The IR absorption analysis of pure drug (MTX), blank NLC formulation (without MTX), and MTX-NLC formulation (MTX loaded) were scanned by FTIR instrument (JASCO International Co. Ltd.; FT-IR 4200; Tokyo; Japan) to detect potential physical interactions. Conventional potassium bromide (KBr) disk or pellet method was used at 1:100 (sample: KBr) ratio, compressed by applying pressure in a hydraulic press. The scanning range for FT-IR measurement was 4000–400  $\text{cm}^{-1}$  operated at a constant resolution of 3  $\text{cm}^{-1}$ .

#### Differential scanning calorimetry (DSC)

DSC thermal analytical technique was used to determine the thermodynamic property of MTX (whether crystalline or amorphous) in the nanoparticles. DSC analysis of MTX, blank (without drug), and lyophilized powders of MTX-NLC was sealed packed in an aluminum pan in Pyris Diamond thermogravimetry/differential thermal analysis (Perkin Elmer, Singapore) instrument at 10°C/min rate of heating and at 30–200°C temperature ranging. The total setup was carried out under nitrogen atmosphere (150 ml/min) protection.

#### Powder X-ray diffraction (PXRD)

The PXRD instrumental investigation of pure MTX powder, lyophilized blank NLC, and optimized MTX-NLC was carried out using a Philips Analytical PXRD spectrometer with Ni-filtered Cu-K $\alpha$  tube source of radiation, operating at 40 kV tube pressure and current of 50 mA. All the samples were analyzed over 5°–40° at 1.3°  $\text{min}^{-1}$  of scanning rate at 2 $\theta$  diffraction angle.

#### Field emission scanning electron microscopy (FESEM) for surface morphology characterization

The surface morphology of the MTX-NLCs was carried out using FESEM (JSM-6700F; Jeol, Tokyo, Japan). Briefly, freeze-dried MTX-NLCs were smoothly spread over a double-sided conductive carbon tape, followed by platinum coating. The images of the samples were then visualized at different magnifications with the aid FESEM at an accelerating 2 kV voltage [32].

#### Transmission electron microscopy (TEM)

TEM analysis of MTX-NLCs was carried out to observe the morphology of the nanocomposites. About 1 mg of the lyophilized MTX-NLC formulation was added to 2 ml of Milli-Q water in an Eppendorf tube, then vortexed and sonicated properly to prevent agglomeration. Then, 4  $\mu\text{l}$  of MTX-NLC suspension was placed on copper grids followed by liquid nitrogen storage until analysis. Finally, TEM images were recorded on a TEM system (JEOL) at 200 kV of acceleration voltage.

#### Lyophilization of MTX-NLCs

To evaluate the efficacy of the formulated NLCs to reconstitute on dehydration, this study was performed. The formulated NLCs were taken in beaker then kept at –30°C for 5 h. The samples were then lyophilized in a lyophilizer (Laboratory Freeze Dryer, Instrument India Ltd., Kolkata, India) at –55°C for 48 h. In the current study, comparative study of the effects of three different types of cryoprotectants (sucrose, mannitol, and lactose) in the concentration of 15% was evaluated. The reconstitution assay was carried out by dispersing the freeze-dried formulations in Milli-Q water and vortexed sufficiently for rehydration of the formulations before further characterization studies.

#### *In vitro* investigations

##### *In vitro* drug release study

The *in vitro* release of MTX from the MTX-NLC composite was determined in medium-like phosphate buffer (pH 7.4) by utilizing

a vertical Franz diffusion cell with a dialysis membrane (HiMedia, Mumbai, India) having molecular weight cutoff range of 12,000–14,000 kDa served as a diffusion membrane [33]. Pieces of the dialysis membrane were soaked in the dissolution media for 24 h before the experiment then tied to the diffusion cell or donor compartment. The receptor compartment was filled with 40 ml of dissolution medium being stirred at 100 rpm and temperature maintained at 37±0.5°C by means of thermostatically maintained water bath. MTX-NLC powder (100 mg) dispersed in 3 ml of the buffer solution was placed in the donor compartment. Aliquots (1 ml) were withdrawn periodically from the receptor compartment which was replaced with an equivalent quantity of fresh medium to maintain the sink condition and assayed by a UV/VIS spectrophotometer (JASCO V-550) at 302 nm. Dissolution experiments were carried out in triplicates.

#### *In vitro* cytotoxicity assessment

The cytotoxicity study of free MTX, MTX encapsulated NLC (MTX-NLC) on breast cancer cell line (MCF7) was evaluated using 3-(4,5-dimethylthiazol-2-yl)-2,5-diphenyl tetrazolium bromide (MTT) assay [34]. The cell lines were obtained from the National Centre for Cell Science, Pune, India. The experiments were performed in 96-well flat bottomed culture plates (BD Biosciences, USA). The cells were placed in each well of the 96-well culture plate with a cell density of 5000 cell/well. MTT was dissolved in phosphate-buffered saline (PBS) at 5 mg/ml. Variable concentrations (0.1–25  $\mu\text{g}/\text{ml}$ ) of free MTX and MTX-loaded NLC were added to each well and incubated for 24 h. After 24 h of incubation with each compound, 20  $\mu\text{l}$  of the MTT dye was added to each 96-well culture plates then kept in an incubator for 4 h at 37°C for the formation of formazan crystals. After incubation, the medium was discarded, then to the formazan crystals, 200  $\mu\text{l}$  of dimethyl sulfoxide was added. The free MTX solution was used as untreated or control group. The absorbance of the soluble formazan dye was measured at 570 nm using a microplate reader. The percentage of viable cells was calculated using the following equation:

$$\text{Cell viability (\%)} = \frac{\text{Absorbance of the treated cells}}{\text{Absorbance of the untreated cells}}$$

#### Cellular uptake analysis using fluorescence imaging

A lipophilic fluorescent dye coumarin 6 (C-6) was used for the analysis of the cellular uptake of MTX in MCF-7 cell lines [35]. MCF-7 cell lines were seeded at a density of 3×10<sup>5</sup> cells/well in 6-well culture plate and incubated overnight inside an incubator for the cell adherence. Then, 1  $\mu\text{g}/\text{ml}$  of C-6 coencapsulated olive oil MTX-NLC and Labrasol® MTX-NLC was added to the plate and incubated for 4 h. Then, the medium was removed and each well was washed thrice with PBS (pH 7.4) and observed under an inverted fluorescence microscope (Carl Zeiss Axio Observer).

#### Stability study

The storage stability of the lyophilized MTX-NLC formulation was determined by studying the changes in PS and EE by storing in different temperatures using DLS. MTX-NLC samples were placed in amber glass vials which were subjected to stability studies as per ICH guidelines. The samples were stored at freezing temperature (2–8°C) and at room temperature inside a desiccator (25±2°C) for a period of 3 months. Samples were analyzed for their physicochemical properties after 30 days, 60 days, and 90 days.

#### Statistical analysis

Statistical analysis was performed using GraphPad Prism software (version 5). Data were expressed as the mean ± standard deviation. Differences for which p<0.05 were considered as statistically significant.

## RESULTS AND DISCUSSION

### Effect of the binary mixture of solid and liquid phase

Solid lipids (Monostearin) to liquid lipids (Labrasol® and olive oil) ratios (90:10, 80:20, 70:30, 60:40, 50:50, and 40:60) were selected randomly.

From the results (Fig. 2a), the entrapment efficiency of both Labrasol® MTX-NLC and olive oil MTX-NLC was enhanced with an increase in the liquid lipid amount. However, when the ratio of solid and liquid lipid was same, there was a sharp decline in the entrapment efficiency. From the groups with low liquid lipid when stored at 4°C, there was expulsion of drug from the NLC composites. Therefore, solid lipid to liquid lipid in the ratio (60:40) was selected as it showed the highest entrapment efficiency due to high lipophilic nature of nanocarrier matrices with no drug expulsion than other groups which could be attributed to the imperfect crystalline arrangement of NLC composite [36].

#### Effect of surfactant concentration on PS and entrapment efficiency

Surfactant plays an important role in the stabilization of NLC composites by reducing the interfacial tension between the dispersed and continuous phase, thereby avoiding coalescence of particles and agglomeration [37]. The NLC formulations were prepared using Poloxamer 188 as surfactants. Poloxamer 188 is a difunctional triblock copolymer surfactant with amphiphilic properties and composed of a hydrophobic block in between two hydrophilic polymer blocks. This property of Poloxamer 188 helps in coating lipophilic nanoparticles and gets adsorbed onto the surface of the NLC composites, thus providing a steric stabilization effect [38]. The effect of the increasing concentration of Poloxamer 188 (1–10% w/w) on PS is illustrated in Fig. 2b. The NLC composites stabilized with 1% w/w Poloxamer 188 showed inefficient stabilization of the formulation. Due to which, the concentration of Poloxamer 188 was increased to 2% w/w which showed reduction in PS, low particle growth was observed in comparison to other concentrations. An increase in surfactant concentration results in thicker coating of NLCs which acts as stronger steric barrier avoiding aggregation and resulting in reduced PS. However, when the concentration of Poloxamer 188 was further enhanced, it resulted in the production of foam. Therefore, 2% w/w of the surfactant was selected as the optimum concentration for the production of NLCs.

#### Physicochemical characterization of the formulated NLCs

##### PS, PDI, and zeta potential of optimized NLC

When the NLCs were assessed by PS analyzer, it showed average PS of  $112.1 \pm 5.6$  for blank NLC (Fig. 3Aa),  $130.2 \pm 4.41$  for olive oil MTX-NLC (Fig. 3Ab), and  $199.6 \pm 1.7$  for Labrasol® MTX-NLC (Fig. 3Ac) with their PDI of  $0.15 \pm 0.02$ ,  $0.21 \pm 0.04$ , and  $0.24 \pm 0.01$ , respectively. The increase in PS and PDI in case of Labrasol® MTX-NLC in comparison to olive oil MTX-NLC may be attributed due to the presence of PEG moieties in Labrasol® which could be extended to the particle surface, leading to increase in particle growth or PS [39]. Surface charge or zeta potential of all the formulations was observed as negative,  $-18.4 \pm 4.8$  mV (blank NLC),  $-24.7 \pm 22$  mV (olive oil MTX NLC), and  $-28.5 \pm 77$  mV (Labrasol® MTX NLC). The diminished zeta potential of Labrasol® MTX-NLC may be attributed due to the presence of PEG chains of Labrasol® covering the particle surfaces.

#### Drug EE% and DL%

The EE% of MTX into formulated NLCs was found equal to be  $95.48 \pm 0.013$  and  $97.25 \pm 0.024$  and DL% was  $9.47 \pm 0.027$  and  $18.48 \pm 0.012$  for olive oil MTX-NLC and Labrasol® MTX-NLC, respectively, which confirms enhanced solubility of drug in the lipid matrices irrespective of the oil-type present ( $p < 0.05$ ) [40].

#### FTIR spectroscopy

The FTIR spectra of pure MTX, blank formulation (blank), and MTX-NLC (Fig. 3B) were quite similar to each other. This shows that there was no significant interaction between MTX and other excipients used in the formulation. FTIR spectrum of pure MTX was showed characteristic peak at  $1446 \text{ cm}^{-1}$ ,  $13384 \text{ cm}^{-1}$ , and  $2936 \text{ cm}^{-1}$  [41]. MTX spectrum showing peak at  $1645 \text{ cm}^{-1}$  indicates the presence of C=C stretching vibration. In terms of the interaction of MTX with excipients, no tangible shift in these four peaks was found indicating the absence of any interaction.

#### DSC

The DSC curve of pure MTX (Fig. 3C) showed a sharp endothermic peak appearing at about  $195^\circ\text{C}$  which corresponds to its melting point and indicating its crystalline nature. The DSC spectra of the MTX-NLC formulation displayed a blunt endotherm at about  $180\text{--}200^\circ\text{C}$  which may be to the change of MTX from crystalline to amorphous form resulting in enhancement of the dissolution profile. DSC characteristic peaks of other two formulations displayed slight differences in the endothermic peak of MTX resulting in no significant physicochemical interaction between MTX and other excipients. The phenomenon of slight shift of MTX in MTX-NLC formulation may be explained as the formation of nanoparticles [42].

#### PXRD

The PXRD patterns of the pure MTX, blank formulation, and MTX-NLC are shown in Fig. 3D. Pure MTX showed diffraction pattern at  $11.35^\circ$ ,  $12.74^\circ$ ,  $14.3^\circ$ ,  $17.5^\circ$ ,  $19.42^\circ$ ,  $23.01^\circ$ , and  $26.93^\circ$  over a diffraction angle of  $2\theta$  indicating a crystalline nature [35], whereas XRD spectra of blank NLC showed loss of peaks and diffused peaks at  $19.25^\circ$ ,  $21.2^\circ$ , and  $23.3^\circ$  which indicate the peaks of excipients used. XRD spectra of MTX-NLC showed peaks at  $19.35^\circ$ ,  $21.5^\circ$ , and  $23.5^\circ$  resulting in shifting of peaks, which suggest the conversion of pure MTX from crystalline to an amorphous state and nearly complete entrapment of the pure MTX in NLC composites which were consistent with the DSC studies.

#### FESEM study

FESEM images of lyophilized Labrasol® MTX-NLC and olive oil MTX-NLC at different magnifications, namely  $\times 30,000$  and  $\times 70,000$  were carried out to determine the shape and size of the NLC composites. The images of olive oil MTX-NLC at  $30,000\times$  magnification (Fig. 4a) and Labrasol® MTX-NLC when captured at  $\times 70,000$  magnification showed that the

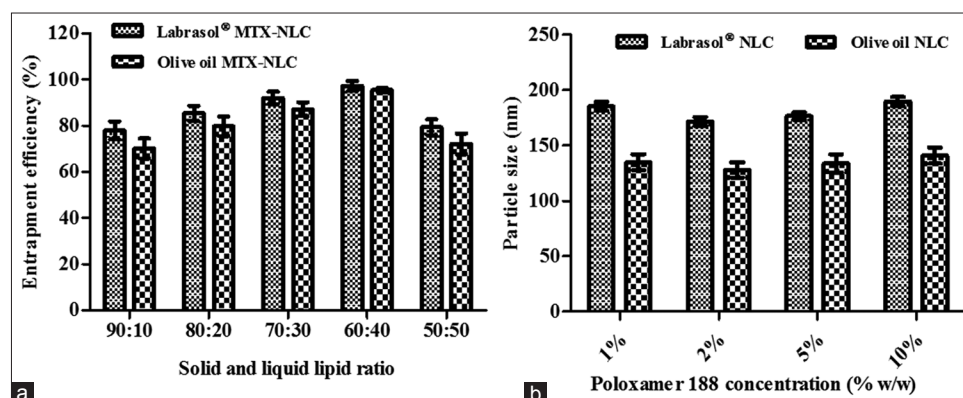


Fig. 2: (a) Effect of different ratios of solid lipid (Monostearin) and liquid lipids (Labrasol® and olive oil) on the entrapment efficiency of the nanostructured lipid carriers (NLCs). (b) Effect of Poloxamer 188 concentration on the particle size of NLCs. Data are represented as mean  $\pm$  standard deviation ( $n=3$ )

NLCs were in nanosize range (100–300 nm) with smooth and distinct spherical structure (Fig. 4b). The average PS of the MTX-NLC correlated well to the values obtained by DLS.

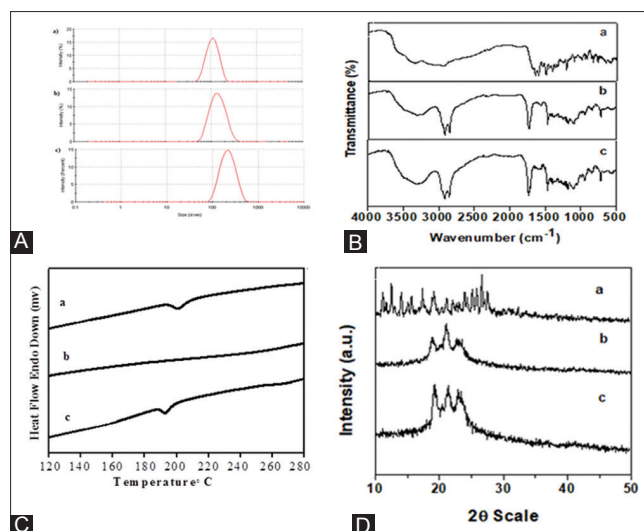


Fig. 3: (A) Size distribution curve of (a) blank-nanostructured lipid carrier (NLC), (b) olive oil methotrexate (MTX)-NLC, (c) Labrasol<sup>®</sup> MTX-NLC. (B) Fourier-transform infrared spectra, (C) differential scanning calorimetry thermograms, and (D) powder X-ray diffraction pattern of (a) MTX, (b) blank formulation, (c) MTX-NLC formulation

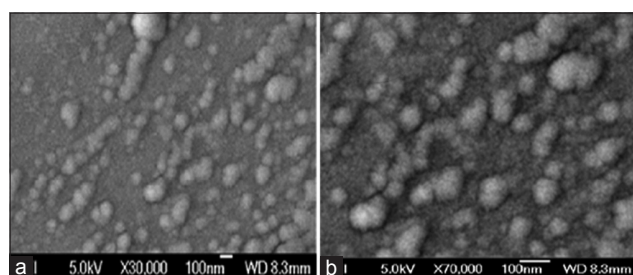


Fig. 4: Field emission scanning electron microscopy images of (a) olive oil methotrexate (MTX)-nanostructured lipid carrier (NLC) at 30,000x magnification (b) Labrasol<sup>®</sup> MTX-NLC at 70,000x magnification

### TEM study

The TEM images obtained were carried out to observe the morphology of the internal structure of the NLCs. MTX-NLCs in both the images showed spherical in shape. TEM image of Labrasol<sup>®</sup> MTX-NLC (Fig. 5b) showed PS larger than that of olive oil MTX-NLC (Fig. 5a), which may be due to the presence of PEG chains present in Labrasol<sup>®</sup>. For passive

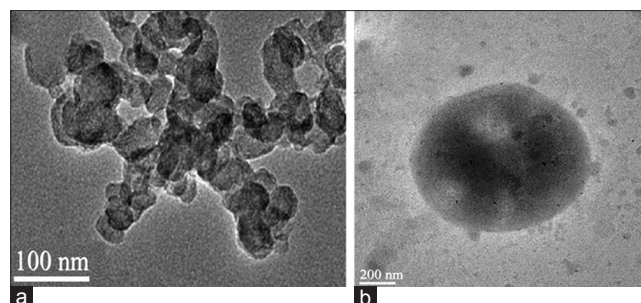


Fig. 5: Transmission electron microscopy images of (a) olive oil methotrexate (MTX)-nanostructured lipid carrier (NLC) (b) Labrasol<sup>®</sup> MTX-NLC

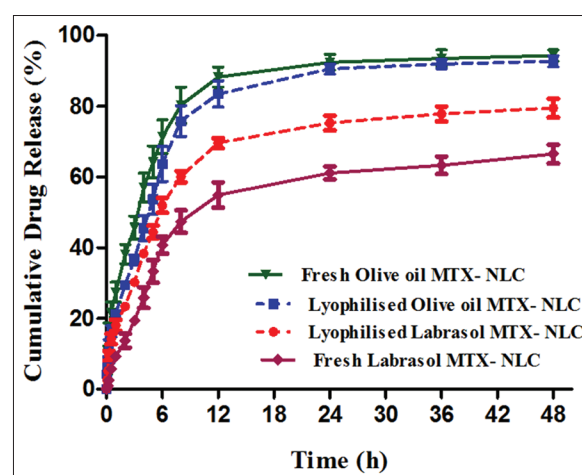


Fig. 6: *In vitro* drug release profiles of fresh olive oil methotrexate (MTX)-nanostructured lipid carrier (NLC), fresh Labrasol<sup>®</sup> MTX-NLC, lyophilized olive oil MTX-NLC, and lyophilized Labrasol<sup>®</sup> MTX-NLC in phosphate buffer pH 7.4. Data are expressed in mean  $\pm$  standard deviation (n=3)

Table 1: PS and PDI of blank NLCs, olive oil NLCs, and Labrasol<sup>®</sup> NLCs before and after lyophilization using sucrose, mannitol, and lactose as cryoprotectants

Formulations	Cryoprotectants (15% w/w)	PS (nm) $\pm$ SD	PDI $\pm$ SD	
Blank NLC	Fresh	112.1 $\pm$ 5.6	0.15 $\pm$ 0.02	
	Lyophilized	Sucrose	120.5 $\pm$ 7.4	0.18 $\pm$ 0.03
		Mannitol	297.37 $\pm$ 7.3	0.29 $\pm$ 0.02
		Lactose	489.24 $\pm$ 3.9	0.45 $\pm$ 0.06
Olive oil MTX-NLC	Fresh	130.2 $\pm$ 4.41	0.21 $\pm$ 0.04	
	Lyophilized	Sucrose	158.9 $\pm$ 7.37	0.26 $\pm$ 0.001
		Mannitol	394.36 $\pm$ 29.30	0.30 $\pm$ 0.05
		Lactose	686.3 $\pm$ 68.40	0.55 $\pm$ 0.009
Labrasol <sup>®</sup> MTX-NLC	Fresh	199.6 $\pm$ 1.7	0.24 $\pm$ 0.01	
	Lyophilized	Sucrose	214.16 $\pm$ 49.2	0.28 $\pm$ 0.008
		Mannitol	463.16 $\pm$ 99.4	0.46 $\pm$ 0.003
		Lactose	847.22 $\pm$ 301.02	0.757 $\pm$ 0.004

All determinations were performed in triplicate and values are expressed as mean $\pm$ SD, n=3. SD: Standard deviation, PDI: Polydispersity index, NLC: Nanostructured lipid carrier, MTX: Methotrexate, PS: Particle size

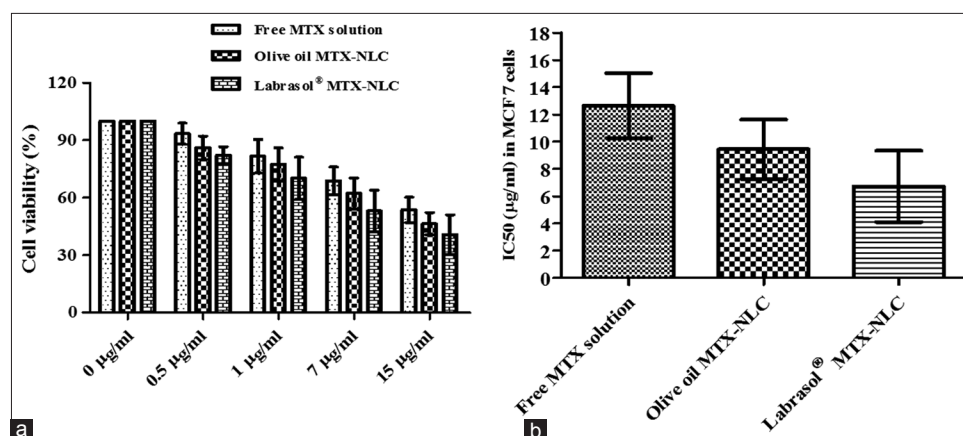


Fig. 7: (a) Cell cytotoxicity effects analysis of free methotrexate (MTX) solution, olive oil MTX-nanostructured lipid carrier (NLC), and Labrasol® MTX-NLC on MCF-7 cells at 24 h using 3-(4,5-di-methylthiazol-2-yl)-2,5-diphenyl tetrazolium bromide assay method. (b) Half maximal inhibitory concentration of free MTX solution, olive oil MTX-NLC, and Labrasol® MTX-NLC formulations in MCF-7 cells. Data are expressed in mean  $\pm$  standard deviation (n=3)

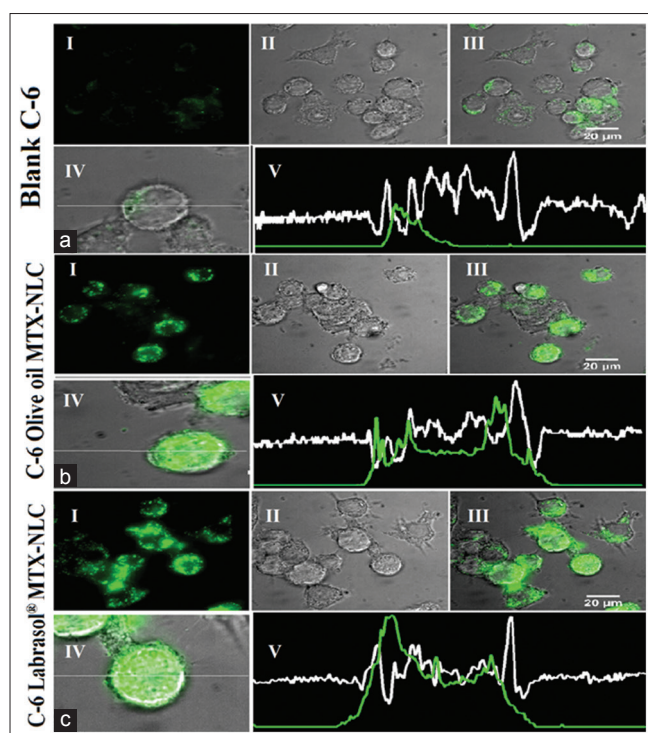


Fig. 8: Cellular uptake analysis of MCF-7 cells incubated for 4 h with (a) blank coumarin-6 (C-6), (b) coumarin-6 (C-6) olive oil methotrexate (MTX)-nanostructured lipid carrier (NLC), and (c) coumarin-6 (C-6) Labrasol® MTX-NLC using inverted fluorescence microscopy imaging. In all the images, (I) corresponds to the images produced in green fluorescence channel, (II) represents the MCF-7 cells differential interface contrast images, (III) is the superimposition of (I) and (II), and (IV) and (V) correspond to the horizontal line series determination of the white and fluorescence line. Scale bar is 20  $\mu$ m

cancer targeting, PS ranging from 100 to 300 nm is considered to be suitable as these particles can easily penetrate into the intracellular space [43]. Due to the presence of PEG chains at the surface of the nanoparticles, the outer layer of Labrasol® MTX-NLC is slightly lighter in color in comparison to olive oil MTX-NLC [44]. Both the TEM results showed PS within the desired range (100–200 nm).

### Lyophilization of MTX-NLCs

One parameter of producing optimized NLCs is to maintaining a stabilized internal structure of the NLC formulation on storage. In general, lyophilized compositions show less aggregations of nanoparticles resulting in more stabilized nanocomposites in comparison to liquid formulations [45]. Different types of cryoprotectants (sucrose, lactose, and mannitol) in the concentration of 15% w/w were evaluated. Initially, 7% w/w concentration was tried which resulted in high PS and PDI. The concentration of cryoprotectants in the range of 10–30% usually produces stable formulations [46]; hence, 15% w/w concentration of cryoprotectants was selected. From the results in Table 1, when 15% w/w sucrose was used, there was slight increase in the PS and PDI in comparison to the fresh formulation which may be due to the disaccharides which reduce the osmotic activity of water and crystallization favoring an amorphous state. Disaccharide lactose lyophilized formulations cause aggregation of particles resulting in enlargement of PS and size distribution [47]. Mannitol lyophilized samples resulted in enlargement in PS and an increase in PDI. Formulations coated with 15% w/w sucrose showed homogeneous PS and improved redispersibility which may be due to the ability of sucrose to interact with polar groups of lipids, and help in stabilizing the membranes after freeze-drying removed by the process of sublimation and therefore used for further lyophilization process.

### In vitro investigations

#### In vitro drug release study

The *in vitro* release profiles of MTX from freshly prepared and lyophilized Labrasol® MTX-NLC and olive oil MTX-NLC are presented in Fig. 6. Release of MTX from the MTX-NLC formulation showed biphasic pattern, burst or fast release at the beginning for a period of about 4–8 h, and sustained release for a period of 48 h. The preliminary burst release of MTX from the MTX-NLC is due to the diffusion of the drug molecules located on the surface of the nanocomposites [48]. It was observed that the cumulative percentage release of all the formulations was significantly different at 8 h ( $p < 0.05$ ). Sustained release of MTX occurs due to the lipophilic nature of the mixture of solid and liquid lipids which acts as a reservoir for the NLCs. The cumulative percentage release from the freshly formulated Labrasol® MTX-NLC (66.45%) was less than that of freshly formulated olive oil MTX-NLC (94.26%). This may be attributed to the presence of the PEG moieties of Labrasol® at the surface of the NLCs causing a barrier for the diffusion of therapeutic moiety to the medium [49]. The lyophilized form of Labrasol® MTX-NLC showed an incremental rise in the cumulative percentage release of MTX (79.46%), whereas the lyophilized form of non-PEGylated olive oil MTX-NLC showed decrease in their cumulative release (92.68%) in comparison to their fresh formulations, respectively. The enhancement

of release from the lyophilized Labrasol® MTX-NLC might be due to the formation of hydrogen bond by the cryoprotectant and the PEG moieties, thereby enhancing the release rate by enabling the surface of the nanoparticle to come in contact with surrounding dissolution medium [45].

#### *In vitro cytotoxicity assessment*

The cytotoxicity study of free MTX solution, olive oil MTX-NLC, and Labrasol® MTX-NLC formulations was carried out by MTT assay against MCF-7 breast cancer cells (Fig. 7). As observed in Fig. 7a, Labrasol® MTX-NLC showed highest cytotoxic response in comparison to olive oil MTX-NLC and free MTX solution. All the formulations showed dose-dependent inhibition effect. As the concentration of MTX was increased, the cytotoxicity was enhanced accordingly in all the cases [50]. Maximum number of cell death was observed in the concentration of 7 µg/ml due to the accumulation of sufficient amount of drug. The half maximal inhibitory concentration (Fig. 7b) value of Labrasol® MTX-NLC was 6.71 µg/ml compared to free MTX solution and olive oil MTX-NLC which was found to be 12.63 µg/ml and 9.45 µg/ml, respectively. These results show that Labrasol® MTX-NLC showed a significant higher cytotoxic effect in comparison to free MTX solution and olive oil MTX-NLC by inhibiting the P-glycoprotein receptors and preventing the efflux of MTX from the cells ( $p < 0.05$ ). This leads to the internalization of MTX in the nuclei of the tumor cells and causing increased cytotoxic effect. These results also confirm that loading MTX into Labrasol® NLC can synergize the cytotoxic efficacy, thereby augmenting its anticancer effect.

#### *Cellular uptake analysis using fluorescence imaging*

The aim of cellular uptake analysis using a fluorescent dye is to know the cellular uptake efficacy of the NLCs into the cells. Microscopic images (Fig. 8) of MCF-7 cells were incubated for 4 h with blank C-6, C-6 olive oil MTX-NLC, and C-6 Labrasol® MTX-NLC. In comparison to the blank C-6, both C-6 olive oil MTX-NLC and C-6 Labrasol® MTX-NLC showed significantly high fluorescence intensity proving higher uptake

and internalization of nanocarriers inside the cytoplasm of the MCF-7 cells. The cellular uptake of NLCs by endocytosis leading to increased intensity of fluorescence also states that MTX will be effectively released from the NLCs in the cellular environment at the desired site of action [51].

#### **Stability study**

In the stability study, irrespective of the type of glyceride presents in the NLC formulations which were stored at freezing temperature and room temperature for 90 days showed minimal variation in PS and entrapment efficiency, thereby maintaining its loose and homogeneous appearance ( $p < 0.05$ ) (Fig. 9). However, after 90 days, increase in PS was more prominent at room temperature than in refrigerated storage conditions. The change in PS was within the acceptable limit of PS for cytotoxics. Therefore, this result suggests that the formulated NLCs were more stable in refrigerated storage temperature than at room temperature to provide an extended half-life period.

#### **CONCLUSION**

In this study, NLCs were formulated using two types of liquid lipids; Labrasol® (PEGylated glyceride) and olive oil (non-PEG lipid) and Monostearin as solid lipid to encapsulate MTX into the formulation. Results obtained from this research work clearly demonstrate that Labrasol® containing NLC composite showed larger PS and substantially provides highest entrapment efficiency with significantly sustained drug release of MTX ( $p < 0.05$ ) from NLCs in pH 7.4 phosphate buffer over 48 h as compared to PEG free olive oil NLC. Furthermore, the formulations were lyophilized using 15% cryoprotectants to improve the stability of the nanocomposites. Results also confirm that Labrasol® MTX-NLC showed the highest cytotoxic response along with prominent cellular uptake. Stability studies confirmed that there was no degradation of nanocomposites on storage at refrigerated and room temperature. Therefore, we conclude that loading of MTX into novel PEGylated glyceride Labrasol® NLC composites can be considered as a promising novel strategy for the delivery of MTX against cancer.

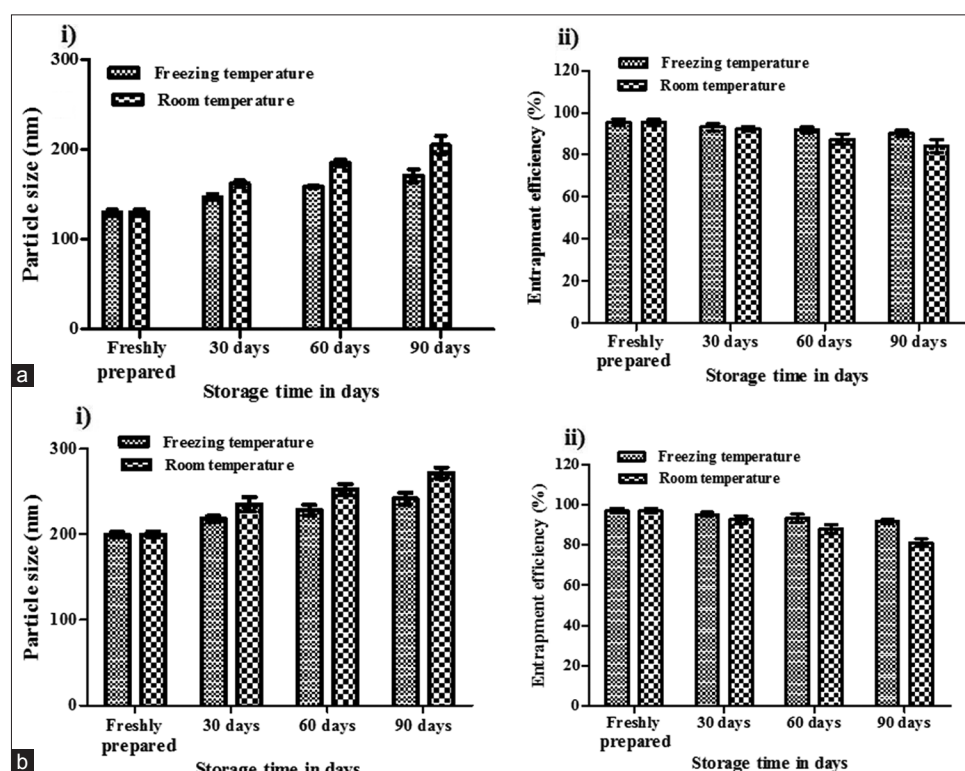


Fig. 9: (i) Particle size (nm) and (ii) drug entrapment efficiency (%) of (a) olive oil methotrexate (MTX)-nanostructured lipid carrier (NLC) and (b) Labrasol® MTX-NLC on storage in freezing temperature and at room temperature for 90 days. Data are expressed in mean  $\pm$  standard deviation ( $n=3$ )

However, these findings are preliminary, future investigations will be on *in vivo* study of these formulations using animal model.

#### ACKNOWLEDGMENT

The authors are thankful to the Department of Pharmaceutical Technology, Jadavpur University, for providing necessary infrastructure and facilities to conduct this research work.

#### AUTHORS' CONTRIBUTIONS

All the authors declare that they have made substantial contributions in design, analysis, interpretation of data, drafting, and revision of the manuscript.

#### CONFLICTS OF INTEREST

The authors declare that there are no conflicts of interest.

#### REFERENCES

- Boyle P, Levin B. World Cancer Report. International Agency for Research on Cancer. Geneva: Distrib by WHO Press Lyon; 2008.
- Siegel RL, Miller KD, Jemal A. Cancer statistics, 2015. *CA Cancer J Clin* 2015;65:5-29.
- Raut I, Doijad R, Mohite S. Solid lipid nanoparticles: A promising drug delivery system. *Int J Pharm Sci Res* 2018;9:862-71.
- Branco MT, Buttros DA, Carvalho-Pessoa E, Sobreira ML, Schincariol CN, Nahas-Neto J, *et al.* Atherosclerotic disease and cardiovascular risk factors in postmenopausal breast cancer survivors: A case-control study. *Climacteric* 2019;22:202-7.
- Abolmaali SS, Tamaddon AM, Dinarvand R. A review of therapeutic challenges and achievements of methotrexate delivery systems for treatment of cancer and rheumatoid arthritis. *Cancer Chemother Pharmacol* 2013;71:1115-30.
- Montaudié H, Sbidian E, Paul C, Maza A, Gallini A, Aractingi S, *et al.* Methotrexate in psoriasis: A systematic review of treatment modalities, incidence, risk factors and monitoring of liver toxicity. *J Eur Acad Dermatol Venereol* 2011;25 Suppl 2:12-8.
- Zhang Y, Chan HF, Leong KW. Advanced materials and processing for drug delivery: The past and the future. *Adv Drug Deliv Rev* 2013;65:104-20.
- Pattni BS, Chupin VV, Torchilin VP. New developments in liposomal drug delivery. *Chem Rev* 2015;115:10938-66.
- Bobo D, Robinson KJ, Islam J, Thurecht KJ, Corrie SR. Nanoparticle-based medicines: A review of FDA-approved materials and clinical trials to date. *Pharm Res* 2016;33:2373-87.
- Zhang L, Gu FX, Chan JM, Wang AZ, Langer RS, Farokhzad OC, *et al.* Nanoparticles in medicine: Therapeutic applications and developments. *Clin Pharmacol Ther* 2008;83:761-9.
- Parveen S, Misra R, Sahoo SK. Nanoparticles: A boon to drug delivery, therapeutics, diagnostics and imaging. *Nanomedicine* 2012;8:147-66.
- Stirling DA. Nanotechnology applications. the nanotechnology revolution. *Pan Stanford* 2018;17:281-434.
- Bertrand N, Wu J, Xu X, Kamaly N, Farokhzad OC. Cancer nanotechnology: The impact of passive and active targeting in the era of modern cancer biology. *Adv Drug Deliv Rev* 2014;66:2-5.
- Wicki A, Witzigmann D, Balasubramanian V, Huwyler J. Nanomedicine in cancer therapy: Challenges, opportunities, and clinical applications. *J Control Release* 2015;200:138-57.
- Eldem T, Speiser P, Hincal A. Optimization of spray-dried and congealed lipid micropellets and characterization of their surface morphology by scanning electron microscopy. *Pharm Res* 1991;8:47-54.
- Müller RH, Radtke M, Wissing SA. Nanostructured lipid matrices for improved microencapsulation of drugs. *Int J Pharm* 2002;242:121-8.
- Forier K, Raemdonck K, De Smedt SC, Demeester J, Coenye T, Braeckmans K, *et al.* Lipid and polymer nanoparticles for drug delivery to bacterial biofilms. *J Control Release* 2014;190:607-23.
- Esposito E, Boschi A, Ravani L, Cortesi R, Drechsler M, Mariani P, *et al.* Biodistribution of nanostructured lipid carriers: A tomographic study. *Eur J Pharm Biopharm* 2015;89:145-56.
- Kapse-Mistry S, Govender T, Srivastava R, Yergeri M. Nanodrug delivery in reversing multidrug resistance in cancer cells. *Front Pharmacol* 2014;5:159.
- Beloqui A, Solinis MÁ, Rodríguez-Gascón A, Almeida AJ, Prést V. Nanostructured lipid carriers: Promising drug delivery systems for future clinics. *Nanomedicine* 2016;12:143-61.
- Thang LQ, Hanh ND, Duong DQ. Study on cause-effect relations and optimization of exemestane-loaded nanostructured lipid carriers. *Int J Pharm Pharm Sci* 2017;9:68-4.
- Tamjidi F, Shahedi M, Varshosaz J, Nasirpour A. Nanostructured lipid carriers (NLC): A potential delivery system for bioactive food molecules. *Innov Food Sci Emerg Technol* 2013;19:29-43.
- Nabi B, Rehman S, Baboota S, Ali J. Insights on oral drug delivery of lipid nanocarriers: A Win-win solution for augmenting bioavailability of antiretroviral drugs. *AAPS PharmSciTech* 2019;20:60.
- Abousamra MM, Mohsen AM. Solid lipid nanoparticles and nanostructured lipid carriers of tolnaftate: Design, optimization and *in vitro* evaluation. *Int J Pharm Pharm Sci* 2015;8:380-5.
- Zhao X, Tang D, Yang T, Wang C. Facile preparation of biocompatible nanostructured lipid carrier with ultra-small size as a tumor-penetration delivery system. *Colloids Surf B Biointerfaces* 2018;170:355-63.
- Grossen P, Witzigmann D, Sieber S, Huwyler J. PEG-PCL-based nanomedicines: A biodegradable drug delivery system and its application. *J Control Release* 2017;260:46-60.
- Tran TH, Ramasamy T, Truong DH, Choi HG, Yong CS, Kim JO, *et al.* Preparation and characterization of fenofibrate-loaded nanostructured lipid carriers for oral bioavailability enhancement. *AAPS PharmSciTech* 2014;15:1509-15.
- Strickley RG. Solubilizing excipients in oral and injectable formulations. *Pharm Res* 2004;21:201-30.
- Rabanel JM, Hildgen P, Banquy X. Assessment of PEG on polymeric particles surface, a key step in drug carrier translation. *J Control Release* 2014;185:71-87.
- Soleimanian Y, Goli SA, Varshosaz J, Sahafi SM. Formulation and characterization of novel nanostructured lipid carriers made from beeswax, propolis wax and pomegranate seed oil. *Food Chem* 2018;244:83-92.
- Kalhapure RS, Sonawane SJ, Sikwal DR, Jadhav M, Rambharose S, Mocktar C, *et al.* Solid lipid nanoparticles of clotrimazole silver complex: An efficient nano antibacterial against *Staphylococcus aureus* and MRSA. *Colloids Surf B Biointerfaces* 2015;136:651-8.
- Dey NS, Mukherjee B, Maji R, Satapathy BS. Development of linker-conjugated nanosize lipid vesicles: A strategy for cell selective treatment in breast cancer. *Curr Cancer Drug Targets* 2016;16:357-72.
- Sahoo RK, Biswas N, Guha A, Sahoo N, Kuotsu K. Development and *in vitro/in vivo* evaluation of controlled release provesicles of a nateginide-maltodextrin complex. *Acta Pharm Sin B* 2014;4:408-16.
- Banerjee P, Geng T, Mahanty A, Li T, Zong L, Wang B, *et al.* Integrating the drug, disulfiram into the vitamin E-TPGS-modified PEGylated nanostructured lipid carriers to synergize its repurposing for anti-cancer therapy of solid tumors. *Int J Pharm* 2019;557:374-89.
- Garg NK, Singh B, Sharma G, Kushwah V, Tyagi RK, Jain S, *et al.* Development and characterization of single step self-assembled lipid polymer hybrid nanoparticles for effective delivery of methotrexate. *RSC Adv* 2015;5:62989-99.
- Iqbal MA, Md S, Sahni JK, Baboota S, Dang S, Ali J, *et al.* Nanostructured lipid carriers system: Recent advances in drug delivery. *J Drug Target* 2012;20:813-30.
- Trotta M, Debernardi F, Caputo O. Preparation of solid lipid nanoparticles by a solvent emulsification-diffusion technique. *Int J Pharm* 2003;257:153-60.
- Bolla PK, Kalhapure RS, Rodriguez VA, Ramos DV, Dahl A, Renukuntla J. Preparation of solid lipid nanoparticles of furosemide-silver complex and evaluation of antibacterial activity. *J Drug Deliv Sci Technol* 2019;49:6-13.
- Yogasundaram H, Bahniuk MS, Singh HD, Aliabadi HM, Uludağ H, Unsworth LD. BSA nanoparticles for siRNA delivery: Coating effects on nanoparticle properties, plasma protein adsorption, and *in vitro* siRNA delivery. *Int J Biomater* 2012;2012.
- Avachat AM, Parpani SS. Formulation and development of bicontinuous nanostructured liquid crystalline particles of efavirenz. *Colloids Surf B Biointerfaces* 2015;126:87-97.
- Garg NK, Tyagi RK, Singh B, Sharma G, Nirbhavane P, Kushwah V, *et al.* Nanostructured lipid carrier mediates effective delivery of methotrexate to induce apoptosis of rheumatoid arthritis via NF-κB and FOXO1. *Int J Pharm* 2016;499:301-20.
- Xia D, Quan P, Piao H, Piao H, Sun S, Yin Y, *et al.* Preparation of stable nitrendipine nanosuspensions using the precipitation-ultrasonication method for enhancement of dissolution and oral bioavailability. *Eur J Pharm Sci* 2010;40:325-34.
- Cooley M, Sarode A, Hoore M, Fedosov DA, Mitragotri S, Gupta AS. Influence of particle size and shape on their margination and wall-

- adhesion: Implications in drug delivery vehicle design across nano-to-micro scale. *Nanoscale* 2018;10:15350-64.
44. Han Y, Zhang Y, Li D, Chen Y, Sun J, Kong F, *et al.* Transferrin-modified nanostructured lipid carriers as multifunctional nanomedicine for codelivery of DNA and doxorubicin. *Int J Nanomedicine* 2014;9:4107-16.
  45. Safwat S, Ishak RAH, Hathout RM, Mortada ND. Nanostructured lipid carriers loaded with simvastatin: Effect of PEG/glycerides on characterization, stability, cellular uptake efficiency and *in vitro* cytotoxicity. *Drug Dev Ind Pharm* 2017;43:1112-25.
  46. Hu FQ, Jiang SP, Du YZ, Yuan H, Ye YQ, Zeng S, *et al.* Preparation and characterization of stearic acid nanostructured lipid carriers by solvent diffusion method in an aqueous system. *Colloids Surf B Biointerfaces* 2005;45:167-73.
  47. Wang Y, Zheng Y, Zhang L, Wang Q, Zhang D. Stability of nanosuspensions in drug delivery. *J Control Release* 2013;172:1126-41.
  48. Zheng D, Dai W, Zhang D, Duan C, Jia L, Liu Y, *et al.* *In vivo* studies on the oridonin-loaded nanostructured lipid carriers. *Drug Deliv* 2012;19:286-91.
  49. Liu Y, Gao D, Zhang X, Liu Z, Dai K, Ji B, *et al.* Antitumor drug effect of betulinic acid mediated by polyethylene glycol modified liposomes. *Mater Sci Eng C Mater Biol Appl* 2016;64:124-32.
  50. Garg NK, Singh B, Jain A, Nirbhavane P, Sharma R, Tyagi RK, *et al.* Fucose decorated solid-lipid nanocarriers mediate efficient delivery of methotrexate in breast cancer therapeutics. *Colloids Surf B Biointerfaces* 2016;146:114-26.
  51. Ying X, Wen H, Lu WL, Du J, Guo J, Tian W, *et al.* Dual-targeting daunorubicin liposomes improve the therapeutic efficacy of brain glioma in animals. *J Control Release* 2010;141:183-92.